Structural, elastic and optical properties of nickel aluminate spinel nano crystalline

K. Adaika*, M. Diaifi, C. Liaidi
University of Biskra, Algeria, Laboratory of Molecular Chemistry and Environment, B.P 14,07000,Algeria

$Ni_{1-x}Cu_xAl_2O_4$nano-crystalline, was made to synthesize by sol–gel method and study their micro-structural, optical and electrochemical properties. All investigated samples were characterized using different techniques such as X-ray diffraction (XRD), Fourier-transform infrared (FTIR) analysis, thermal gravimetric analysis (TG), and transmission electron microscope (TEM), optical absorption and electrochemical measurements. Powder X-ray diffraction (XRD) analysis was confirmed the formation of single phase, cubic spinel structure without other impurities. Average crystallite sizes of the samples were found to be in the range of 44 nm to 57 nm by Scherrer's method. FT-IR spectra showed the stretching frequencies corresponding to the M–Al–O bond of spinel structure. The SEM micrographs suggest homogeneous distribution of the nanocrystallites in the samples. The optical band decreases with increasing copper substitution from 2.41 to 1.98 eV. The study of electrochemical behavior shows that the electrode with large copper content has a better electrocatalytical activity.

(Received February 13, 2021, Accepted May 24, 2021)

*Keywords:*Nickel aluminate, Spinel, Sol gel method

1. Introduction

Nickel aluminate ($NiAl_2O_4$) is a ternary oxide with AB_2O_4 spinel structure, where A and B are cations occupying tetrahedral (Ni^{2+} and octahedral (Al^{3+} sites, respectively[1]. Due to its high mechanical resistance, as well as its high thermal and chemical stabilities, nickel aluminate has been employed as catalyst support in various chemical reactions such as partial oxidation of methane to syngas[2], CO_2 reforming of methane, chemical-looping combustion, acetylene hydrogenation, steam reforming of methane, combustion of methaneand k2steam reforming of glycerol to hydrogen production. $NiAl_2O_4$ particles have been prepared by various routes such as sol-gel[3], solid state reaction, microwave[1] [4], Pechini method[5], thermal decomposition of polynuclear malate complexes, mechano-chemical synthesis, one-pot processand combustion route[6]. In this work, we propose the use of an alternative route the sol-gel for the preparation of $Ni_{1-y}Cu_yAl_2O_4$spinels, results in the generation of a material with porous structure and high surface area[7], which are very important properties for catalytic and adsorptive purposes.

In the present work, we have successfully substituted tetrahedrally coordinated Ni^{2+} ions by Cu^{2+}ions and obtained hole-rich $Ni_{1-y}Cu_yAl_2O_4$(y =0.0-1.0).

The objective of this work was to investigate the influence of substitution on the thermal treatment, the physical characteristicsof nickel aluminate oxide obtained by use of sol-gel as precursor.

2. Experimental

Copper substituted nickel aluminate $Ni_{1-y}Cu_yAl_2O_4$, where y =0, 0.25, 0.75, 1.0. Were prepared by sol-gel method assisted by citric acid acting as the chelat agent. Nickel nitrate hexahydrate, Copper nitrate hexahydrate, Aluminate nitrate and citric acid monohydrate are the raw elements which are taken in the stoichiometric amounts. These raw materials are mixed

* Corresponding author: K.adaika@univ-biskra.dz

thoroughly and dissolved in de-ionized water. The mixing and dissolving is done in their molar ratio of 1:1. The solution is continuously stirred for 4 h at 90 °C. This resulted in a homogeneous solution. This homogeneous solution is vaporized at 100 °C till a dry gel is formed. The obtained gel is ground and calcinated for 5 h at 1000 °C to decompose the nitrates phase identification and the calculation of the amount of each phase present were carried out using XRD analysis. The patterns were recorded at room temperature using (D8 Advance Bruker diffractometer) equipped with Cu-Kα radiation (λ = 0.15406 nm) . Measurements were achieved for 2θ angles in the 10-90° range, by step of 0.02 °.The optical absorption spectra were measured by a SHIMADZU UV-2550 spectrophotometer at room tempera-ture, with a deuterium lamp for UV and a tungsten halogen lamp for the visible region.

3. Results and discussion

3.1. Differential thermal analysis

TG and DTA curves of the thermal degradation of the Nickel aluminate precursor powder are shown in Fig. 1. The TG pattern shows that, there is a weight loss at 127 °C, 254 °C, and 410 °C, with an overall weight loss of 36%. The first two weight loss steps represent the loss of physisorbed and interlayer water, respectively [8]. The third weight loss has been attributed to the loss of structural water, CO_2, and NH_3 from the interlayer because of the destruction of layered structure [9]. The DTA pattern of the precursor shows irreversible broad endothermic peaks at 257 °C and 362 °C. Also, it shows exothermic peaks at 206 °C, 302 °C and 432 °C. A broad exothermic feature around 445 °C indicates the crystallisation of $Ni_{1-y}Cu_yAl_2O_4$ spinel. At temperatures higher than 445°C, the mass loss is insignificant, and the crystallinity of oxyds is increased.

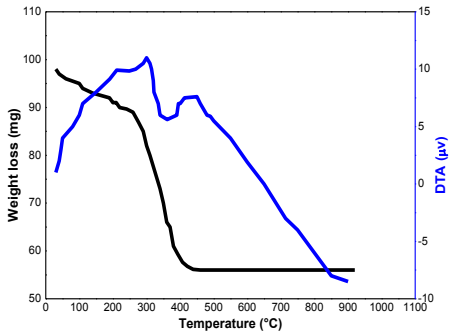

Fig.1.TG-and-DTA-diagrams of gel $Ni_{1-y}Cu_yAl_2O_4$heated in air at 10 °C/min.

3.2. X – ray diffraction analysis

X-ray diffraction analysis performed on samples thermally treated at 1000 °C , are illustrated in Fig.2. The peaks located at 2**θ** of 18.04°, 30.20°,35.41°,43.45°, 53.74°,57.65° and 63.08° are assigned to the (111), (220), (311), (400), (422), (511) and (440) planes of the cubic spinel structure of $Ni_{1-y}Cu_yAl_2O_4$ respectively (JCPDF file 10-0339). The patterns indicate that all samples are well crystalized, with the cubic majority phase of spinel. According to the results presented in [11] the arrangement of the $NiAl_2O_4$ structure, begins at 900°C. The peaks are sharp and narrower implying the high crystalline nature of the synthesized materials. Moreover the peaks shift towards the higher value of 2**θ** as the concentration of Cu^{2+} decrease and hence confirming a increasing lattice parameter .The results show that the lattice parameter a slightly increases with Cu^{2+} doping content are shown in Table 1.Th increase of a with y can be explained on the basis of the difference in ionic radius of Ni^{2+} and Cu^{2+}.The smaller ionic radius of Ni (0.69Å) was replaced by the larger ionic radius of Cu (0.73Å) so the lattice parameter increased due to the expansion of the unit cell.

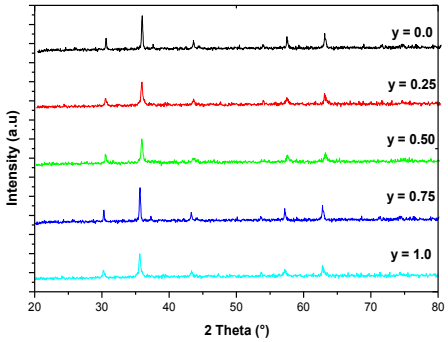

Fig.2.XRD patterns of the $Ni_{1-y}Cu_yAl_2O_4$ (y =0.0-1.0) powders calcined at 1000 °C.

The particles sizes are also determined using the maximum peak from the XRD pattern (311) by the Debye Scherrer' formula [11].

$$D = \frac{0.9\lambda}{\beta\cos\theta} \quad (1)$$

where D is the crystallite size (nm), λ is the wavelength of X-ray radiation source (1.5406 Å for CuKα), ß istheintegral width, and θ is the peak position. The values of D are reported in Table 1.

Table 1. Average crystallite size (D), lattice parameter (a) of the $Ni_{1-y}Cu_yAl_2O_4$spinels.

Samples	D(nm)	a (Å)	Unit cells volume ($Å^3$)
$NiAl_2O_4$	44	8.0451	520.7081
$Ni_{0.75}Cu_{0.25}Al_2O_4$	51	8.0482	521.3103
$Ni_{0.5}Cu_{0.5}Al_2O_4$	53	8.0771	526.9463
$Ni_{0.25}Cu_{0.75}Al_2O_4$	54	8.0778	527.0833
$CuAl_2O_4$	57	8.0803	527.5729

3.3. FTIR Spectroscopy analysis

The typical transmittance FT-IR spectra of $Ni_{1-y}Cu_yAl_2O_4$ powders are shown in Fig.3 as a series of transmission peaks in the range of 400–4000 cm^{-1}.

FT-IR analysis was performed to investigate the formation of metal aluminate spinel structure.

The characteristic bands appear at around 590,670 cm^{-1}, which would confirm the formation of $Ni_{1-y}Cu_yAl_2O_4$ aluminate spinel structure, in good agreement with the XRD results [12,13]. These bands can be attributed to the symmetric stretching, bending, and asymmetric stretching modes ofNi–O, Al–O, and Ni–O–Al bonds at tetrahedral and octahedral sites in metal aluminate spinels [14-16].

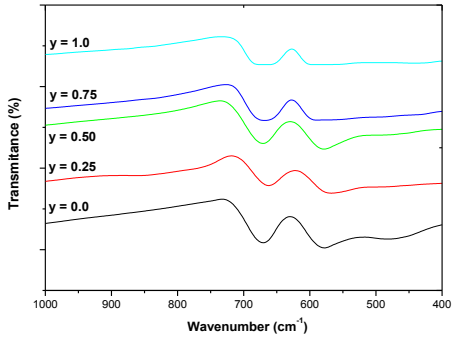

Fig.3. Infrared spectra of $Ni_{1-y}Cu_yAl_2O_4$ calcined at 1000 °C.

3.4. Elastic properties

The force constant K for tetrahedral site K_t and octahedral site K_o were calculated employing the method suggested by Waldron [17]. According to Waldron, the force constants for tetrahedral A-sites (K_t) and octahedral B-sites (K_o) are given by:

$$K_t = 7{,}62.M_1.\upsilon_1^2.10^{-7} \quad \text{N/m} \quad (2)$$

$$K_o = 5.31.M_2.\upsilon_2^2.\ .10^{-7} \quad \text{N/m} \quad (3)$$

where M_1 and M_2 are the molecular weight of A and B site respectively, υ_1 is the corresponding center frequency of tetrahedral site where as υ_2 is the corresponding center frequency of octahedral site. The values of force are summarized in Fig. 4. It can be seen that, k_t and K_o increases as y increases. Furthermore the calculated values of k_t are greater than those of the corresponding values of k_o. However the values of the bond length of A-site (R_A) are smaller than those of B-site (R_B). This is due to the inverse proportionality between the bond length and the force constants [18].

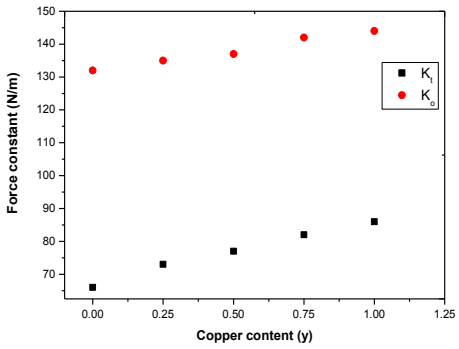

Fig.4. The effect of composition on the variation oftetrahedral and octahedral force constants (k_t and K_o).

Analysis of IR spectra with crystallographic knowl-edge helps us to determine the Debye temperature and elastic properties. The Debye temperature ($\boldsymbol{\theta}_D$) of all samples was calculated using the wave number of IR bands [19].

$$\theta_D = \frac{\square Cvav}{k} \quad (4)$$

where h = h/2π , k is the Boltzmann constant, C is velocity of light (c = 3×10^8 cm/s), and υ_{av} is the average wavenumber of bands. The values of the Debye temperature for $Ni_{1-y}Cu_yAl_2O_4$ samples

are shown in Fig.5.It is observed that the Debye temperature increase with increasing Cu^{2+} content.The observed increase in Debye temperature (θ_D) with copper concentration (y) suggested that lattice vibrations are hindered due to Ni-substitution.

This may be due to the fact that strength of interatomic bonding increases with concentration (y) as supported by our results on the variation of of elastic moduli.

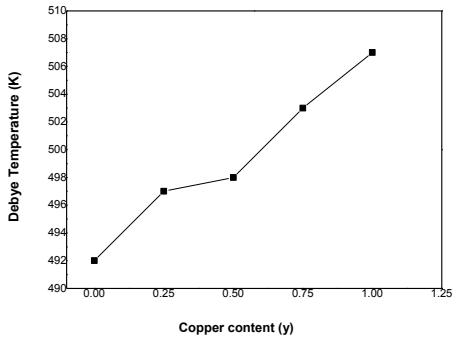

Fig. 5. Variation of Debye temperature calculated withCu content.

For an isotropic material the values of Stifness constants (C_{11} and C_{12}) can be determined by utilizing X-ray and FTIR data. Velocity of longitudinal (V_l), transverse elastic wave (V_t), mean elastic velocity (V_{av}), rigidity modulus (G), Poisson's ratio (P) and Young's modulus (E) were calculated andregistered in Table 2.

$$C_{11} = C_{12} = \frac{Kav}{a} \quad (5)$$

$$B = \frac{1}{3}[C_{11} + 2C_{12}] \quad (6)$$

$$V_l = \left(\frac{C_{11}}{\mathrm{dx}}\right)^{1/2} \quad (7)$$

$$\mathrm{V_t} = \frac{\mathrm{V_l}}{\sqrt{3}} \quad (8)$$

$$V_{av} = \frac{1}{3}\left[\frac{2}{{V_l}^3} + \frac{1}{{V_t}^3}\right]^{-1/3} \quad (9)$$

$$G = d_x V_t^2 \quad (10)$$

$$P = \frac{(3B-2G)}{(6B+2G)} \quad (11)$$

$$E = (1+p)2G \quad (12)$$

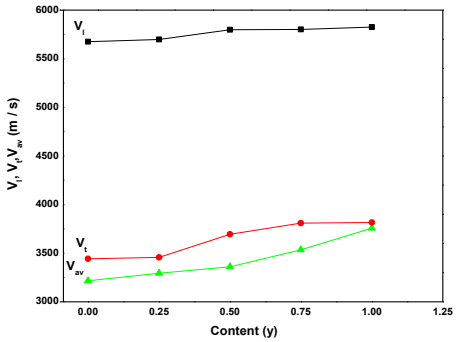

Fig.6. Variation of Velocity of longitudinal (V_l), transverse elastic wave (V_t) and mean elastic velocity (V_{av}), with Cu content.

Fig.6 shows the shear and longitudinal sound velocity respectively as a function of Cu ion concentration. It can be seen that the general trend is the increase of the sound velocity with increasing Cu^{2+} ion concentration.

It can be seen that values of E and G in Fig.7 are slightly increasing with increase in the y value.

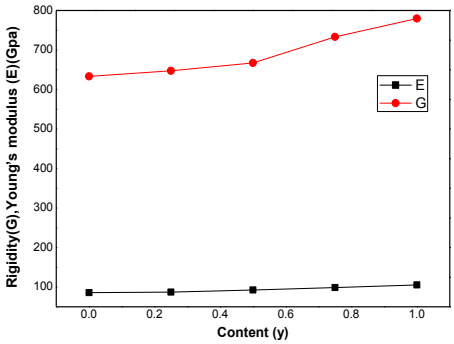

Fig.7.Rigidity (G) and Young's modulus of $Ni_{1-y}Cu_yAl_2O_4$ aluminate.

The increases in elastic moduli may be due to the inter-atomic binding between various atoms in the spinel lattice. When strength of inner atomic bonding increases, elastic moduli also increases as nickel (Ni) atoms are replaced by copper (Cu) atoms. The magnitudes of Poisson's ratio (P) were found to be constant (P = 0.35) for all samples, which is consistent with the theory of isotropic elasticity [20].

Table 2.Longitudinal elastic wave, transverse elastic wave, mean elastic velocity, rigidity modulus (G), Young's modulus (E), and Debye temperature of $Ni_{1-y}Cu_yAl_2O_4$ aluminate.

Sample	**V_l(m/s)**	**V_t(m/s)**	**V_{av}(m/s)**	**θ (K)**	**G (Gpa)**	**E (Gpa)**
y=0.0	5675.29	3443.12	3216.33	492	633.35	85.65
y=0.25	5698.32	3456.65	3293.34	497	647.15	87.35
y=0.5	5798.03	3695.25	3360.26	498	667.45	92.37
y=0.75	5800.90	3809.47	3535.26	503	733.22	98.65
y=1.0	5825.12	3816.28	3756.95	507	779.5	105.45

3.5. Optical absorpk8tion

Fig.8 illustrates the UV–vis absorbance spectra of $Ni_{1-y}Cu_yAl_2O_4$ aluminate calcined at 1000°C.

All the spectra display a common feature: a strong absorption band can be observed from 540 to 650 nm, which is within the visible region (400–780 nm). The absorption peak at ~493 nm is influenced by the spin forbidden $^4A2(F)\rightarrow{}^2T(G)$ transition of Ni^{2+} ions in octahedral positions of spinel structure [21]. The spin allowed $^4A2\text{-}(F)\rightarrow 4T1(P)$ transition of Ni^{2+}ions in tetrahedral sites can be observed from 580 to 680 nm.The absorption band observed at 790 nm is probablycharacteristic of the transition $^6A_{1g}\rightarrow{}^4T_{2g}$ as Cu^{2+} octahedral [22]. This result confirms that the ions cu^{2+} was incorporated into $NiAl_2O_4$ by substituting some of the existing Al^{3+} ions in the octahedral sites.

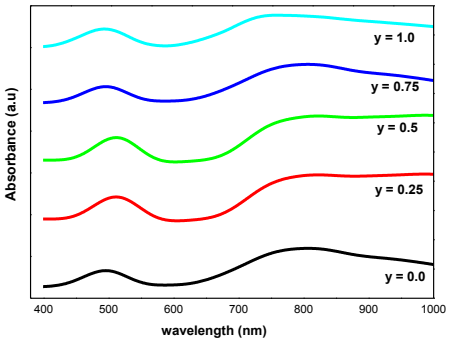

Fig.8.UV–vis absorbance spectra of $Ni_{1-y}Cu_yAl_2O_4$ aluminate calcined at 1000°C.

The values of the optical gap (Eg) of $Ni_{1-y}Cu_yAl_2O_4$ are determined from the measurement of the reflectance by UV–Vis diffused reflectance. The band gap can be determined by extrapolation to the energy axis of the linear plots $(\alpha h\nu)^n$as a function of the photon energy (hν). To determine the type of transition, we have used the Tauc formula:

$$(\alpha h\nu)^m = A(h\nu - Eg) \qquad (13)$$

whereα represent the absorption coefficient and A constant, respectively.The exponent m takes the value 2 for a direct transition and 1/2 for an indirect transition.The band gap obtained from the plot of (αhν)2 versus hν and listed in Table 3. The Eg values are found to decrease rapidly as y increases with Cu-substitution. This decrease can be attributed to the induced deep defects levels following the Cu doping. Therefore, the Cu-substituted NiAl2O4 can absorb more photons and generate more electron and holes, which is favorable for a higher photocatalytic activity compared to the unsubstituted compounds (NiAl2O4, CuAl2O4) with 2.37 and 2.04 eV of band gap energy (Eg), respectively. The Eg results agree with those reported in the literature for $NiAl_2O_4$and $CuAl_2O_4$ [23].

Table 3.The values of the optical gap (Eg) of $Ni_{1\ y}Cu_yAl_2O_4$.

Sample	Eg (eV)
$NiAl_2O_4$	2.41
$Ni_{0.75}Cu_{0.25}Al_2O_4$	1.89
$Ni_{0.5}Cu_{0.5}Al_2O_4$	1.54
$Ni_{0.25}Cu_{0.75}Al_2O_4$	1.52
$CuAl_2O_4$	1.98

4. Conclusions

In the present work, nickel aluminate spinel was prepared by sol-gel method. The formation of nickel aluminate phase was confirmed by XRD and FT-IR. It was found that the lattice parameter increased from 8.0451Å to 8.0803 Å as the Cu^{+2} concentration increased which obeyed Vegard's law. The main absorption bands of spinel aluminate appeared through IR absorption spectra recorded in the range of 400-1000 cm^{-1}. The elastic properties of aluminate with Cu^{+2} were interpreted in terms of binding forces.

References

[1] Y.S. Han, J.B. Li, X.S. Ning, X.Z. Yang, B. Chi, Mat. Sci. Eng. A.**369**,241 (2004).
[2] R. López-Fonseca, C. Jiménez-González, B. Rivas, J.I. Gutiérrez-Ortiz, Appl. Catal. A Gen. **53**, 437 (2012).
[3] C.O. Areán, M. P. Mentruit, A.J.L. López, J.B. Parra, Coll. Surf. A: Physicochem. Eng. Aspects **180**,253 (2001).
[4]R.D. Peelamedu, R. Roy, D. K. Agrawal, Mater. Lett.**55**, 234 (2002).
[5]L. Gama, M.A. Ribeiro, B.S. Barros, R.H.A. Kiminami, I. T. Weber, A.C.F.M. Costa, J. Alloys Compds. **483**,453 (2009).
[6] E. Leal, A.C.F.M. Costa, N.L. Freita, H.L. Lira, R. H.G.A. Kiminami, L. Gama, Mater. Res. Bull.**46**, 1409 (2011).
[7] G.D. B. Nuernberg, E.L. Foletto, L.F.D. Probst, C.E. M. Campos, N.L.V. Carreño, M.A. Moreira, Chem. Eng. J. **21**, 193 (2012).
[8] K. Rida, M.A. Pena, E. Sastre, A. Martinez-Arias, J. Rare Earths. **30**, 210 (2012).
[9] M. Marciuš, M. Ristic, M. Ivanda, S. Music, J. Alloys. Compd. **541**, 238 (2012).
[10] I. Lazau, C. Corcoveanu, C. Pacurariu, R.I. Lazau, Romanian Journal of Materials **43**, 425 (2013).
[11] A. Becheri, M. Durr, P. Lo Nostro, P. Baglioni, J. Nanopart.Res.**10**, 679 (2008).
[12] R. Samkaria, V. Sharma, Mater SciEng B.**178**, 1410 (2013).
[13] G.Buvaneswari, V. Aswathy, R. Rajakumari, Dye Pigment. **123**, 413 (2015).
[14] F. Davar, M. Salavati-Niasari, J AlloysCompd.**509**, 2487 (2011).
[15] D. L. Ge, Y. J. Fan, C. L. Qi et al.,J Mater Chem A.**1**, 1651 (2013).
[16] W. Staszak, M. Zawadzki, J. Okal,J Alloys Compd.**492**, 500 (2010).
[17] R. D. Waldron, Physical Review**99**(6), 1727 (1955).
[18] S. C. Watawe, B. D. Sutar, B. D. Sarwade, B. K. Chougule, International Journal of Inorganic Materials**3**(7), 819 (2001).
[19] S.A. Mazen, S.F. Mansour, E. Dhahari, H.M. Zaki, T.A. Elmosalami, J. AlloysCompd. **470**,294 (2009).
[20] K.B. Modi, J. Mater. Sci. **39**(8), 2887 (2004).
[21] X. Duan, M. Pan, F. Yu et al., J. Alloys Compd.**509**, 1079 (2011).
[22] N.Pailhe, A.Wattiaux, M. Gaudon, A. Demourgues, J. Solid State Chem.**181**, 1040 (2008).
[23] I. Sebai, N. Salhi, G.Rekhila, M. Trari, V Int. J. Hydrogen Energy.**42**, 26652 (2017).